Topological Tuning in Three-Dimensional Dirac Semimetals

Awadhesh Narayan[*]

School of Physics and CRANN, Trinity College, Dublin 2, Ireland

Domenico Di Sante[†]

Consiglio Nazionale delle Ricerche (CNR-SPIN), Via Vetoio, L'Aquila, Italy
and Department of Physical and Chemical Sciences, University of L'Aquila,
Via Vetoio 10, I-67010 L'Aquila, Italy

Silvia Picozzi

Consiglio Nazionale delle Ricerche (CNR-SPIN), Via Vetoio, L'Aquila, Italy

Stefano Sanvito

School of Physics, CRANN and AMBER, Trinity College, Dublin 2, Ireland

We study with first-principles methods the interplay between bulk and surface Dirac fermions in three dimensional Dirac semimetals. By combining density functional theory with the coherent potential approximation, we reveal a topological phase transition in $Na_3Bi_{1-x}Sb_x$ and $Cd_3[As_{1-x}P_x]_2$ alloys, where the material goes from a Dirac semimetal to a trivial insulator upon changing Sb or P concentrations. Tuning the composition allows us to engineer the position of the bulk Dirac points in reciprocal space. Interestingly, the phase transition coincides with the reversal of the band ordering between the conduction and valence bands.

Introduction.—In recent years an ever growing attention has been devoted to Dirac fermions, both in two as well as in three dimensions. The fabrication of graphene and topological insulators has motivated a surge of investigations in this field [1–3]. Acting as a possible bridge between the two, recently Dirac semimetals in three dimensions were theoretically proposed [4]. Using first-principles calculations, Wang and co-workers predicted sodium bismuthate (Na_3Bi) and cadmium arsenide (Cd_3As_2) to be three dimensional Dirac semimetals [5,6]. Their experimental realization has not been far behind and the prediction verified by means of angle resolved photoemission measurements in a remarkably rapid flurry of activity by a number of groups [7–11]. Interestingly, a Dirac semimetal state was also found in zinc blende compounds [12]. Apart from hosting a bulk Dirac cone, both Na_3Bi and Cd_3As_2 also show a band inversion at the center of the Brillouin zone (BZ). This means that they exhibit a surface Dirac spectrum when confined to a slab geometry, analogously to conventional topological insulators [13]. Given their unique electronic structure, this class of compounds opens up an exciting platform to study topological phase transitions, interweaving two- and three-dimensional Dirac states.

In this Letter, we study the interplay of surface and bulk Dirac states by using first-principles density functional theory (DFT) and *ab initio* derived tight-binding models. Based on our first-principles calculations, we predict that the bulk Dirac cone of Na_3Bi is formed only for films with a thickness larger than 90 nm, while the surface Dirac state, originating from a bulk band inversion, becomes gapless for films with a thickness as small as 4.5 nm, up to an energy resolution of ≈ 3 meV (a resolution accessible by the most recent state-of-the-art spectrometers [14]). Furthermore, by employing the coherent potential approximation joint with DFT, we uncover a topological phase transition in the $Na_3Bi_{1-x}Sb_x$ and $Cd_3[As_{1-x}P_x]_2$ alloys. We propose a means to engineer the k-space position of the bulk Dirac point by changing the Sb or P concentrations. At the critical Sb (P) concentration of $\approx 50\%$ ($\approx 10\%$), this crossing reaches the BZ center, meeting its time-reversed partner, whereupon they annihilate and render the bulk gapped. This topological phase transition is accompanied by a simultaneous loss of the inverted band character. Beyond the critical Sb (P) concentration, the alloy is adiabatically connected to the topologically trivial Na_3Sb (Cd_3P_2).

Computational methods.—We have carried out first-principles calculations by using the projector augmented plane wave method as implemented in Vienna *ab initio* simulation package (VASP) [15], and employed the Perdew-Burke-Ernzerhof parametrization of the exchange-correlation functional [16]. Spin orbit coupling was included for all computations in a self-consistent manner. The electronic structure simulations have been performed with a plane wave cutoff of 600 eV on an $8 \times 8 \times 4$
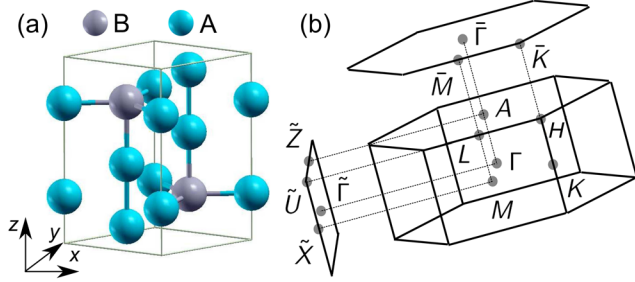
FIG. 1 (color online). (a) Hexagonal unit cell for A_3B compounds, with $A =$ Na, K, Rb and $B =$ Bi, Sb. (b) Bulk and surface projected Brillouin zone for the structure with the high symmetry points marked. The three dimensional Dirac crossing occurs along the $\Gamma - A$ direction.

Monkhorst-Pack k-point mesh. All the A_3B compounds ($A =$ Na, K, Rb, $B =$ Bi, Sb) investigated here crystallize in the D_{6h}^4 structure, as shown in Fig. 1. During the structural optimization the atomic coordinates were allowed to relax until total energy differences were less than 1 meV. From the bulk first-principles results, we have projected onto a basis of Na $3s$ and Bi $6p$ (Sb $5p$) orbitals by using a procedure based on constructing Wannier functions [17]. The obtained tight-binding parameters were then used to study slab geometries. By combining this scheme with a coherent potential approximation (CPA) including self-energy corrections for disorder, we have investigated the $Na_3Bi_{1-x}Sb_x$ alloy [18]. We note that this methodology has been recently used to predict the robustness of Dirac fermions in topological crystalline insulator (TCI) alloys, as well as in ferroelectric Rashba semiconductor (FERSC) alloys [19].

Results and discussions.—We begin our analysis by calculating the relativistic bulk band structures for the four materials Na_3Sb, Na_3Bi, K_3Bi, and Rb_3Bi, as shown in Fig. 2. For Na_3Bi we find the three dimensional Dirac

crossing along the $\Gamma - A$ line, and a band inversion at the BZ center, which is consistent with the previous study of Wang *et al.* [5]. Na_3Sb, in contrast, is a small gap insulator with a conventional band ordering. Our calculations reveal that on replacing Na in Na_3Bi with heavier atoms, the resulting compounds K_3Bi and Rb_3Bi are metallic with small electron pockets around Γ. However, the crossing away from Γ is still present. The band structures for the two materials are shown in Figs. 2(c) and 2(d), along with a zoom around the BZ center in the insets. A transition from a hexagonal to a cubic form has been reported for K_3Bi and Rb_3Bi at high temperatures [20,21]. So, our results for the band structures of these two materials are expected to hold at low temperatures.

Since Na_3Bi also shows an inverted band character around the Fermi level, one expects it to form surface states when confined into a two-dimensional geometry, similar to a topological insulator. Therefore, we study the evolution of the spectrum of Na_3Bi films oriented along the [010] surface, as a function of their thickness. For thicknesses ranging from 1 to 4 layers, the films are gapped due to an interaction between the two surfaces, as shown in Fig. 3(a). This gap decreases monotonically, with the surface cone at $\tilde{\Gamma}$ becoming gapless for a 5-layer-thick film. One can also notice the shoulder along the $\tilde{\Gamma} - \tilde{Z}$ direction, which rises upwards in energy to form the bulk Dirac crossing for thicker films. This bulk crossing is fully formed only for film thicknesses larger than 100 layers (≈ 90 nm). We note that the surface Fermi arcs can exist with the bulk Dirac nodes, as long as the two-dimensional $\mathbb{Z}_2$ invariant on the $k_z = 0$ plane, ν_{2D}, is nontrivial [22]. Our predictions for the thickness dependence of the surface and bulk Dirac cones call for verifications by angle resolved photoemission experiments. Indeed, such measurements with varying film thickness have been recently
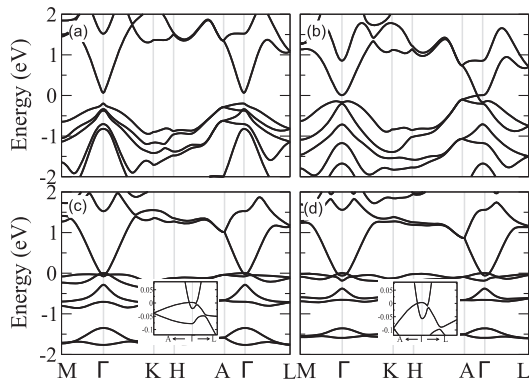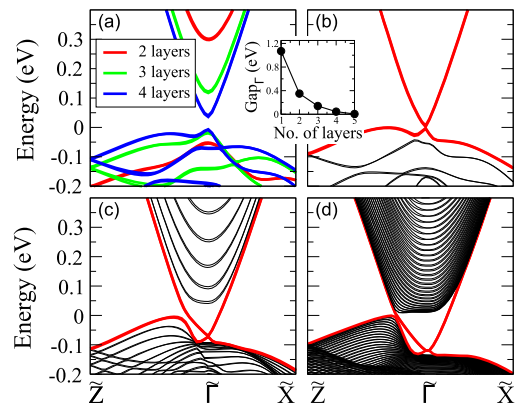

FIG. 2. Bulk band structures obtained by including spin orbit interaction for (a) Na_3Sb, (b) Na_3Bi, (c) K_3Bi, and (d) Rb_3Bi. Note the Dirac crossing in (b)–(d). The insets in (c) and (d) show a zoom around Γ with the crossing along $\Gamma - A$.

FIG. 3 (color online). Band structures for Na_3Bi thin films of thickness (a) 2–4 layers, (b) 5 layers, (c) 20 layers, and (d) 100 layers. Inset in (a)–(b) shows the energy gap at the center of the Brillouin zone for slabs of thickness 1 to 5 layers. In (b)–(d) Dirac crossings are highlighted in red (gray).
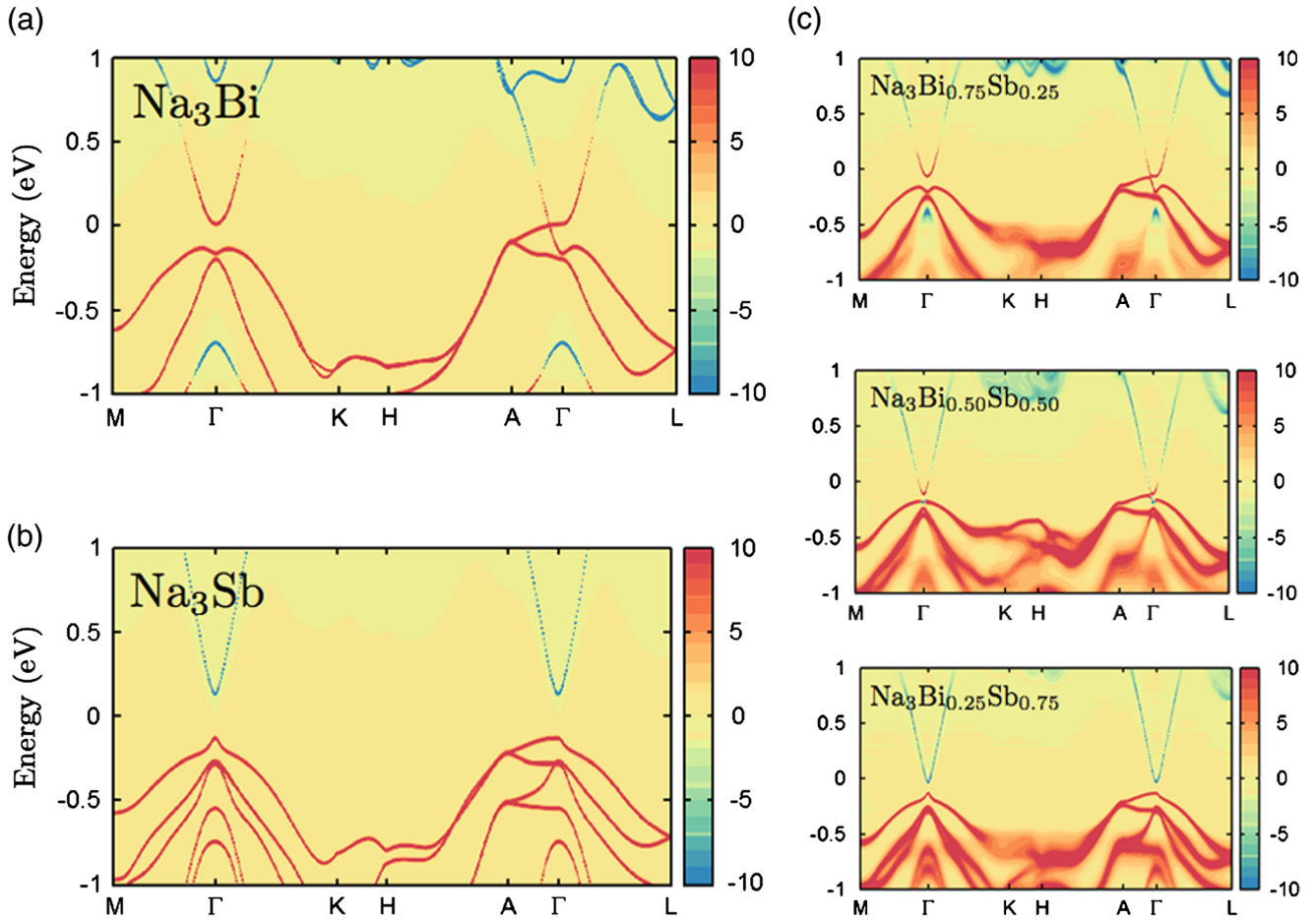
FIG. 4 (color online).   Spectral functions for pristine (a) Na_3Bi and (b) Na_3Sb. (c) Spectral functions for the $Na_3Bi_{1-x}Sb_x$ alloy with increasing Sb concentration ($x = 0.25, 0.50, 0.75$ from top to bottom). The color scale shows the orbital contribution, with red (dark gray, positive values) denoting the Bi/Sb p orbitals and blue (light gray, negative values) representing the Na s orbital (in units of states/eV).

undertaken for topological insulator films [23,24]. In the case of Na_3Bi [010] slabs, one should be able to see two gap-closing transitions at very different film thicknesses: one for the surface cone for a few layers slab, with the next gap closing occurring in the bulk for a hundred layers slab. For the [001] surface, the bulk and surface Dirac cones are all projected onto the Brillouin zone center. In contrast, these Dirac crossings are separated in reciprocal space for the [010] surface. We decided to focus on the latter, as in this case it may be easier to distinguish the two cones in an angle-resolved photoemission measurement. Very recently, thin films of Na_3Bi have been grown by molecular beam epitaxy [25], a development which provides a clear route to verify our predictions.

We now turn our attention to the $Na_3Bi_{1-x}Sb_x$ alloy. From the bulk band structures in Fig. 2, we observe that Na_3Sb is topologically trivial, having neither the bulk Dirac crossing nor a band inversion at the BZ center, as opposed to Na_3Bi. This opens up the intriguing possibility to obtain a quantum phase transition in $Na_3Bi_{1-x}Sb_x$ solid solutions.

To this end, we have performed DFT + CPA calculations for the alloy. The spectral functions at different Sb concentrations are shown in Fig. 4. With increasing Sb concentration, the bulk Dirac crossing along $\Gamma - A$ moves towards the BZ center. At around a critical concentration of $x_c = 0.5$ ($Na_3Bi_{0.5}Sb_{0.5}$), this crossing reaches close to Γ. Upon subsequent increase in Sb concentration, an energy gap appears. We note that this is the consequence of the annihilation between this Dirac cone and its time-reversed partner along the Γ to $-A$ direction. The Sb concentration therefore represents an efficient tool to manipulate the position of the bulk Dirac points in k space along the $\Gamma - A$ line. Interestingly, the disappearance of the bulk cone is accompanied by a loss of the inverted band character, as it can be evidenced from the reversal in orbital character of the valence and conduction bands, before and after passing through the critical Sb concentration. From bulk-boundary correspondence, one can then infer that for slabs made of these alloys there would also be a transition in the surface spectrum: below x_c the surface would display a Dirac

crossing, while increasing Sb concentration beyond this value would lead to the opening of a trivial gap. Thus, our calculations reveal a topological phase transition in the prototypical three-dimensional Dirac semimetal.

Recently, such tunable phase transitions were experimentally reported for topological insulators and topological crystalline insulators [26–29]. This makes us confident that our predictions can be verified in the near future. It is also worthy considering that our DFT + CPA calculations reveal a protection against substitutional disorder of the spectral features of three-dimensional Dirac semimetals around the Fermi level. We note, in fact, the absence of broadening of spectral features around the cone, as compared to other energies. Such a robustness, similar to what happens for topological crystalline insulators and Weyl fermion systems, arises from the three-dimensional nature of the Dirac cone [19], and in turn leads to the concrete possibility of experimental verifications by means of spectroscopic techniques. As shown in Ref. [19], this is a consequence of a vanishing disorder self-energy around the crossing point. We also propose that a similar phase transition, and a similar robustness against disorder, would occur in the $Cd_3(As_{1-x}P_x)_2$ alloy, since the parent compounds Cd_3As_2 and Cd_3P_2 are Dirac semimetal and conventional insulator, respectively, with the former having an inverted band order and the latter having a normal band sequence (see Supplemental Material [30]).

Conclusions.—In summary, we have studied the interplay between bulk and surface Dirac fermions in prototypical three dimensional Dirac semimetals, by using first-principles-based tight-binding calculations. Furthermore, by means of density functional theory with coherent potential approximation simulations, we have revealed a topological phase transition in $Na_3Bi_{1-x}Sb_x$ and $Cd_3[As_{1-x}P_x]_2$. The change of Sb or P concentration provides an efficient way to engineer the reciprocal space position of the three dimensional Dirac cone, with potential implications for technological devices benefiting from this additional degree of freedom. Intriguingly, the phase transition from a Dirac semimetal to an insulator is accompanied by a change in the bulk band ordering. This can be related, via the bulk-boundary correspondence, to a concomitant transition in the surface state spectrum.

*narayaa@tcd.ie
†domenico.disante@aquila.infn.it

[1] A. K. Geim and K. S. Novoselov, Nat. Mater. **6**, 183 (2007).
[2] M. Z. Hasan and C. L. Kane, Rev. Mod. Phys. **82**, 3045 (2010).
[3] X.-L. Qi and S.-C. Zhang, Rev. Mod. Phys. **83**, 1057 (2011).
[4] S. M. Young, S. Zaheer, J. C. Y. Teo, C. L. Kane, E. J. Mele, and A. M. Rappe, Phys. Rev. Lett. **108**, 140405 (2012).
[5] Z. Wang, Y. Sun, X.-Q. Chen, C. Franchini, G. Xu, H. Weng, X. Dai, and Z. Fang, Phys. Rev. B **85**, 195320 (2012).
[6] Z. Wang, H. Weng, Q. Wu, X. Dai, and Z. Fang, Phys. Rev. B **88**, 125427 (2013).
[7] Z. K. Liu, B. Zhou, Y. Zhang, Z. J. Wang, H. M. Weng, D. Prabhakaran, S.-K. Mo, Z. X. Shen, Z. Fang, X. Dai, Z. Hussain, and Y. L. Chen, Science **343**, 864 (2014).
[8] S.-Y. Xu *et al.*, arXiv:1312.7624.
[9] Z. K. Liu, J. Jiang, B. Zhou, Z. J. Wang, Y. Zhang, H. M. Weng, D. Prabhakaran, S.-K. Mo, H. Peng, P. Dudin, T. Kim, M. Hoesch, Z. Fang, X. Dai, Z. X. Shen, D. L. Feng, Z. Hussain, and Y. L. Chen, Nat. Mater. **13**, 677 (2014).
[10] M. Neupane *et al.*, Nat. Commun. **5**, 3786 (2014).
[11] S. Borisenko, Q. Gibson, D. Evtushinsky, V. Zabolotnyy, B. Buchner, and R. J. Cava, Phys. Rev. Lett. **113**, 027603 (2014).
[12] M. Orlita, D. M. Basko, M. S. Zholudev, F. Teppe, W. Knap, V. I. Gavrilenko, N. N. Mikhailov, S. A. Dvoretskii, P. Neugebauer, C. Faugeras, A.-L. Barra, G. Martinez, and M. Potemski, Nat. Phys. **10**, 233 (2014).
[13] H. Zhang, C.-X. Liu, X.-L. Qi, X. Dai, Z. Fang, and S.-C. Zhang, Nat. Phys. **5**, 438 (2009).
[14] A. Damascelli, Phys. Scr. **T109**, 61 (2004).
[15] G. Kresse and J. Furthmuller, Comput. Mater. Sci. **6**, 15 (1996).
[16] J. P. Perdew, K. Burke, and M. Ernzerhof, Phys. Rev. Lett. **77**, 3865 (1996).
[17] A. A. Mostofi, J. R. Yates, Y.-S. Lee, I. Souza, D. Vanderbilt, and N. Marzari, Comput. Phys. Commun. **178**, 685 (2008).
[18] P. Soven, Phys. Rev. **156**, 809 (1967).
[19] D. Di Sante, P. Barone, E. Plekhanov, S. Ciuchi, and S. Picozzi, arXiv:1407.2064.
[20] D. E. Sands, D. H. Woods, and W. J. Ramsey, Acta Crystallogr. **16**, 316 (1963).
[21] Chuntonov *et al.*, Sov. Phys. Crystallogr. **22**, 367 (1977).
[22] B.-J. Yang and N. Nagaosa, Nat. Commun. **5**, 4898 (2014).
[23] Y. Zhang *et al.*, Nat. Phys. **6**, 584 (2010).
[24] M. Neupane *et al.*, Nat. Commun. **5**, 3841 (2014).
[25] Y. Zhang, Z. Liu, B. Zhou, Y. Kim, Z. Hussain, Z.-X. Shen, Y. Chen, and S.-K. Mo, Appl. Phys. Lett. **105**, 031901 (2014).
[26] S.-Y. Xu, Y. Xia, L. A. Wray, S. Jia, F. Meier, J. H. Dil, J. Osterwalder, B. Slomski, A. Bansil, H. Lin, R. J. Cava, and M. Z. Hasan, Science **332**, 560 (2011).
[27] T. Sato, K. Segawa, K. Kosaka, S. Souma, K. Nakayama, K. Eto, T. Minami, Y. Ando, and T. Takahashi, Nat. Phys. **7**, 840 (2011).
[28] P. Dziawa *et al.*, Nat. Mater. **11**, 1023 (2012).
[29] S.-Y. Xu *et al.*, Nat. Commun. **3**, 1192 (2012).
[30] See Supplemental Material at http://link.aps.org/supplemental/10.1103/PhysRevLett.113.256403 for CPA calculations for the $Cd_3(As_{1-x}P_x)_2$ alloy, along with a low-energy model to study the topological phase transition.